



Article

Determination of the Effective Lifetime of a Spinor Bose–Einstein Condensate

Xin Wang¹, Yong Qin¹, Jun Jian¹, Wenliang Liu^{1,2,*}, Jizhou Wu^{1,2,*} , Yuqing Li^{1,2}, Vladimir Sovkov^{1,3} 
and Jie Ma^{1,2}

- ¹ State Key Laboratory of Quantum Optics Technologies and Devices, Institute of Laser Spectroscopy, Shanxi University, Taiyuan 030006, China; 202222607065@email.sxu.edu.cn (X.W.); 202222607051@email.sxu.edu.cn (Y.Q.); 202212603006@email.sxu.edu.cn (J.J.); lyqing2006@sxu.edu.cn (Y.L.); v.sovkov@spbu.ru (V.S.); mj@sxu.edu.cn (J.M.)
- ² Collaborative Innovation Center of Extreme Optics, Shanxi University, Taiyuan 030006, China
- ³ St. Petersburg State University, 7/9 Universitetskaya nab., St. Petersburg 199034, Russia
- * Correspondence: liuwl@sxu.edu.cn (W.L.); wujz@sxu.edu.cn (J.W.)

Abstract: The effective lifetime of ultra-cold atoms in specific quantum states plays a crucial role in studying interaction parameters within quantum systems. Measuring the effective lifetime of various quantum states within ultra-cold atoms is a fundamental task in quantum operations. In this paper, the effective lifetimes of the excited electronic states $|F = 2, m_F = -2\rangle$, $|F = 2, m_F = -1\rangle$, and $|F = 2, m_F = 0\rangle$ for a sodium atomic Bose–Einstein condensate (BEC) are investigated in both the optical dipole trap (ODT) and one-dimensional optical lattice. Through the analysis of experimental data, we demonstrate the significant advantage of lattice loading over the optical dipole trap in terms of atomic lifetimes. The results provide crucial insights into the temporal scales relevant for investigating the evolution of boson gases in optical lattices, facilitating the realization of quantum simulations pertaining to unique quantum phases, and providing an important experimental basis for the research of non-equilibrium dynamics between different spin states.

Keywords: effective lifetime; ultra-cold atoms; optical dipole trap; optical lattice



Received: 14 November 2024

Revised: 14 January 2025

Accepted: 29 January 2025

Published: 30 January 2025

Citation: Wang, X.; Qin, Y.; Jian, J.; Liu, W.; Wu, J.; Li, Y.; Sovkov, V.; Ma, J. Determination of the Effective Lifetime of a Spinor Bose–Einstein Condensate. *Photonics* **2025**, *12*, 124. <https://doi.org/10.3390/photonics12020124>

Copyright: © 2025 by the authors. Licensee MDPI, Basel, Switzerland. This article is an open access article distributed under the terms and conditions of the Creative Commons Attribution (CC BY) license (<https://creativecommons.org/licenses/by/4.0/>).

1. Introduction

Bose–Einstein condensates (BECs) have attracted considerable attention in recent years due to their noteworthy macroscopic quantum properties. Rapid advancements in experimental techniques have facilitated the successful realization of quantum gases for a diverse range of atomic species by physicists [1–3]. The effective lifetime of atoms is a crucial parameter in BEC-based experiments. Additionally, the precision of quantum measurements, the fidelity of quantum gates, and the operational scope of quantum simulations are all directly or indirectly related to the effective lifetime of atoms. Extending the atomic lifetime facilitates the deployment of advanced and nuanced quantum manipulation techniques. The precise determination of the effective lifetime of atoms and the extension of their lifespan through quantum manipulation have been the subject of extensive interest from researchers [4–9].

Remarkable achievements in both experimental and theoretical fields regarding the effective lifetime of atoms have emerged, such as alkali-metal Rydberg atoms, molecules formed in mixtures of ultra-cold atoms, and atoms confined in optical tweezers or optical lattices. The continuous advancement of experimental techniques and theoretical research

has led to remarkable achievements in the study of the lifetime of cold atoms. In 1996, C.W. Oates et al. measured the lifetime of the Na $3p^2P_{3/2}$ state to be 16.237(35)ns through precise spectroscopy of optically prepared ultra-cold two-level atoms [10]. In 1998, J.E. Simsarian et al. detected the decay of fluorescence in ^{210}Fr atoms by exciting atoms in a magneto-optical trap (MOT). This provided the most accurate experimental test of the many-body perturbation theory for the heaviest alkali metal [11]. Later, the lifetime constrained by a heating effect in 1D optical lattices was investigated [12]. The research provided experimental guidance for the design of long-lived optical lattices. In 2013, Sophie Pelisson et al. investigated variations in the lifetimes of atoms trapped in an optical lattice in proximity to a surface, showing that the presence of the surface introduces boundary conditions that only slightly alter the value of the ordinary Wannier–Stark lifetimes [13]. In 2015, Erhan Saglamyurek and colleagues studied the hole storage lifetime in the ground-state electronic Zeeman sublevels of erbium, which can last up to 30 seconds [14]. It should be noted that the lifetimes in various Rydberg states have been accurately measured using pulsed-field ionization technology and all-optical methods [15,16]. Meanwhile, the effect of ambient temperature changes due to black-body radiation on the lifetimes of the Rydberg states has been researched [16–21]. In addition, the lifetimes of complex molecules have been experimentally proven [22,23]. Interestingly, the lifetimes of both single atoms and alkaline-earth circular Rydberg atoms captured in optical tweezer arrays, as well as the lifetimes of d -band ultra-cold atoms in one-dimensional and triangular optical lattices, have recently been reported [24–27].

The spinor BEC demonstrates a significant degree of spin freedom. When combined with microwaves, radio-frequencies, and various other modulation techniques, the excited electronic states of the spinor BEC in this optical environment serve as excellent candidates for investigating quench dynamics, phase transition phenomena, and many-body physics [28–34]. To facilitate these quantum manipulations, it is crucial to determine the effective lifetime of the excited electronic state. However, research on the lifetime of the excited electronic states of the spinor BEC in both the optical dipole trap (ODT) and optical lattice has yet to be reported.

In this paper, the coherent coupling between the $|F = 1, m_F = -1\rangle$ state and the $|F = 2\rangle$ state of the Na spinor BEC is successfully achieved through a microwave pulse. Furthermore, we measure the effective lifetime of the excited electronic spin states $|F = 2\rangle$ in both the optical dipole trap and the one-dimensional optical lattice. Our research provides valuable insights for the efficient quantum manipulation of ultra-cold Na spinor BECs and promotes the development of complex quantum simulation experiments as well as the study of dynamical behavior and interaction characteristics between atoms in different states.

2. Experimental Setup and Results

The preparation of ultra-cold Na BECs can be found in our previous work [35]. The experiments were carried out in a vacuum cell. The atomic beam from the oven was decelerated by the Zeeman slower and captured through an MOT. The atom cloud was further cooled by the compressed magneto-optical trap and optical molasses process, loaded into a crossed optical dipole trap composed of two 1064 nm laser beams, and vaporized to prepare the final BEC. As illustrated in Figure 1a, the pink crossed beams represent the two dipole trap beams. The angle between the two crossed beams was 45° , and the beam waists were $32\ \mu\text{m}$ and $39\ \mu\text{m}$, with a power of 15.6 W and 12.0 W, respectively [35]. Finally, information on atoms in different spinor components was precisely acquired through absorption imaging and digital analyses.

After evaporative cooling, the atoms in the BEC were held in the ODT, with trap frequencies of 361 Hz in the radial direction and 341 Hz in the longitudinal direction. By optimizing the gradient magnetic field, we obtained a pure-state $|F = 1, m_F = -1\rangle$ BEC with 2×10^5 Na atoms at a temperature of about tens of nK [36]. A microwave pulse was employed to facilitate a coherent transition between the $|F = 1, m_F = -1\rangle$ state and the different Zeeman sublevels of the $|F = 2\rangle$ state. The microwave pulse was generated by a microwave source (SRS, SG386), amplified by a power amplifier (30 W, mini-circuits, ZHL-30W-252-S+), and finally transmitted through a microwave chip (TAOGLAS PC104R.A.07.0165C). The switching of the microwave pulse was controlled by a switch (mini-circuits, ZASW-2-50DR+), which can modulate microwave signals quickly with a remarkable response speed of up to 50 ns. As a result, the coherent transitions from the $|F = 1, m_F = -1\rangle$ state to the electronic states $|F = 2, m_F = -2\rangle$, $|F = 2, m_F = -1\rangle$, and $|F = 2, m_F = 0\rangle$ were achieved by tuning the frequency and amplitude of the microwave. In our experiment, the microwave amplitudes required to achieve transitions from the ground state to the $|F = 2, m_F = -2\rangle$, $|F = 2, m_F = -1\rangle$, and $|F = 2, m_F = 0\rangle$ Zeeman sublevels were all 0 dBm, and the frequencies were 1.768964 GHz, 1.769852 GHz, and 1.770738 GHz, respectively.

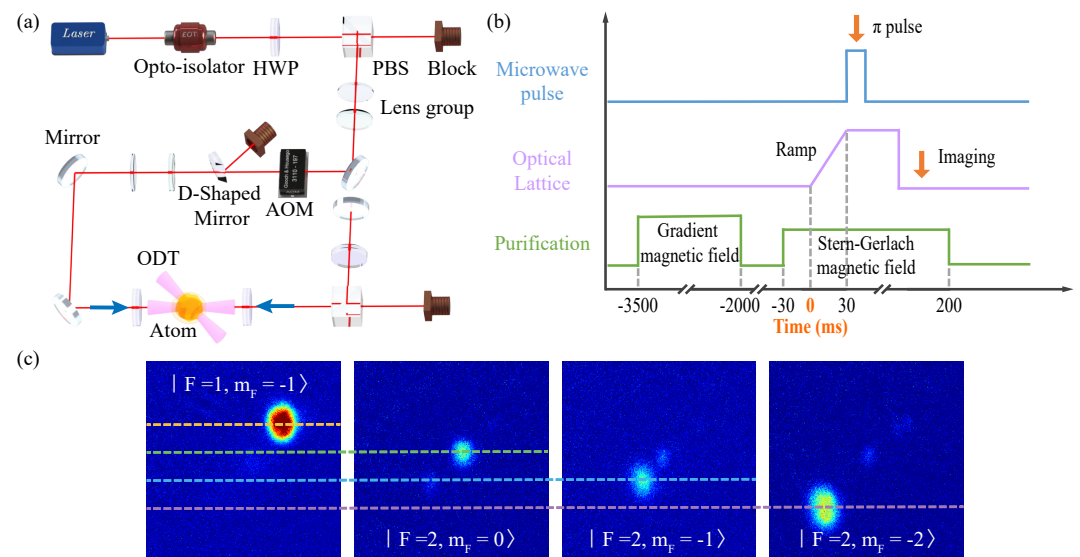


Figure 1. (a) Schematic of the optical lattice and the optical dipole trap (ODT). The red line indicates the beam path of the lattice laser. A pair of opposite blue arrows represent two laser beams forming the one-dimensional optical lattice. Crossed beams at the atomic cloud represent the ODT. HWP: half-wave plate; PBS: polarizing beam splitter; AOM: acousto-optic modulator. (b) Schematic of the experimental time sequence. The horizontal axis is not scaled proportionally. (c) Images of atomic cloud distribution for different Zeeman states.

2.1. Lifetime of BECs in an Optical Dipole Trap

The ODT plays a pivotal role in the experimental system, where the final evaporative cooling and the realization of the BEC occur. After achieving the purified $|F = 1, m_F = -1\rangle$ state BEC in the ODT, we applied different microwaves to the initial state atoms to couple them to the $|F = 2, m_F = 0\rangle$, $|F = 2, m_F = -1\rangle$, and $|F = 2, m_F = -2\rangle$ states. Subsequently, all trapped beams were switched off, allowing the atoms to fly freely and undergo absorption imaging. Figure 1c illustrates the atomic cloud states where atoms were excited to different Zeeman sublevels. We measured the number of atoms in the trap at various hold times. The normalized data for the lifetimes of the excited electronic states $|F = 2, m_F = -2\rangle$, $|F = 2, m_F = -1\rangle$, and $|F = 2, m_F = 0\rangle$ are shown in Figure 2.

The experimental data presented in Figure 2 indicate that the number of atoms decays with the hold time. In accordance with the definition of the effective lifetime, as presented in Ref. [27], the time for the fitting curve to decrease to the e^{-1} of the initial atomic number was taken as the effective lifetime, τ_0 , corresponding to the time at the intersection of the curve and the dashed line shown in Figure 2. The decay of the atomic number in the trap can be expressed as [12,15,21,27]

$$N = N_0 \exp\left(-\frac{t}{\tau_1}\right) + \delta n_0, \quad (1)$$

where N represents the normalized number of atoms, t represents the hold time, and the constants N_0 , τ_1 , and δn_0 represent the amplitude, time constant, and offset, respectively. As the hold time increased, the number of atoms trapped in the well continuously decayed due to factors such as mutual collisions between atoms and spontaneous emission. In our experiment, the time constants for the $|F = 2, m_F = -2\rangle$, $|F = 2, m_F = -1\rangle$, and $|F = 2, m_F = 0\rangle$ states were 0.508 ± 0.031 ms, 0.604 ± 0.030 ms, and 7.336 ± 0.345 ms, respectively. According to the fitting results, the effective lifetimes of the $|F = 2, m_F = 0\rangle$ and $|F = 2, m_F = -1\rangle$ states were approximately 0.844 ms and 0.781 ms. The number of atoms in the $|F = 2, m_F = -2\rangle$ state remained stable for a hold time of up to 4 ms. The effective lifetime derived from the exponential curve fitting to the atomic number was approximately 12.302 ms. When comparing the effective lifetimes of the atoms in these three states, it is evident that the effective lifetime of the $|F = 2, m_F = -2\rangle$ state was significantly longer than those of the other two states.

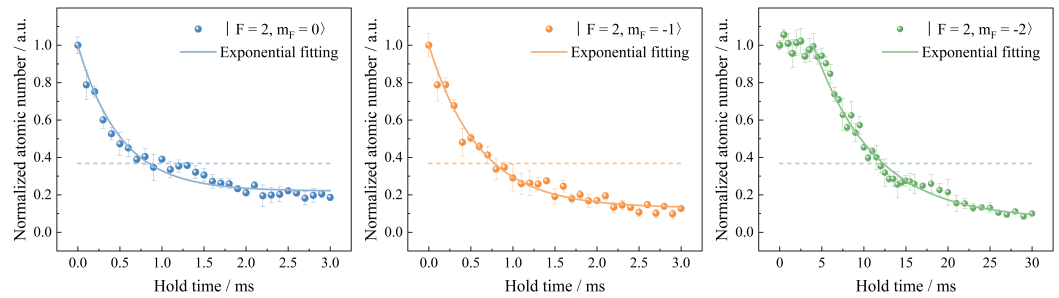


Figure 2. The lifetimes of the excited electronic states $|F = 2, m_F = 0\rangle$, $|F = 2, m_F = -1\rangle$, and $|F = 2, m_F = -2\rangle$ are shown. The differently colored dots represent the experimental results, while the curves represent the results of exponential curve fitting. The dashed lines indicate the positions where the number of atoms drops to e^{-1} of the initial atomic number. The time at the intersection of the dashed line and the solid curve signifies the lifetime of the atoms in the corresponding energy state.

2.2. Lifetime of the $|F = 2, m_F = 0\rangle$ State in a One-Dimensional Optical Lattice

In this section, we investigate the influence of lattice depth on the effective lifetime in a one-dimensional optical lattice. The purity and controllability of optical lattices provide an ideal platform for quantum simulation with ultra-cold atomic systems. It should be noted that we only investigate the lifetime of the $|F = 2, m_F = 0\rangle$ state in the optical lattice, as its effective lifetime in the ODT is the shorter.

One-dimensional optical lattices are formed by a pair of counter-propagating coherent laser beams, creating a periodic optical potential well with a period equal to half the wavelength of the laser used to form the lattice [37]. In Figure 1a, the thin red lines represent the actual beam path of the lattice beam, which overlaps with one arm of the optical dipole trap. A red-detuned 1064 nm fiber laser (ALS-IR-1064, 30W) served to form the optical lattice. A pair of opposite blue arrows represents the incident and reflected beams, the coherent interference between them creates an ordered crystal structure, namely the optical lattice. In our experimental setup, the frequency of the lattice laser is red-detuned relative

to the atomic transition, and the atoms are trapped in the lattice at the points of maximum laser intensity. The depth of the lattice was varied by adjusting the lattice laser power. The experimental sequence is shown in Figure 1b. The gradient magnetic field was used to purify the spinor sodium BEC to $|F = 1, m_F = -1\rangle$ state. The Stern–Gerlach magnetic field was employed to spatially separate the Zeeman states, thereby enabling the observation of distinct quantum states. The purple line represents the optical lattice loading. When the power of the lattice beam was ramped up to a preset value, the microwave, indicated by the blue line, began to transfer the atoms from the initial state ($|F = 1, m_F = -1\rangle$) to the final state ($|F = 2, m_F = 0\rangle$). The number of atoms in the $|F = 2, m_F = 0\rangle$ state was detected at different hold times using the same method as in the ODT.

Considering the potential influence of phase transitions from superfluid to Mott insulator states within the optical lattice on the effective lifetime of atoms, we determined that the lattice depth at which phase transitions occur was approximately 13.7 Er under the experimental conditions [38]. All measurements in this study were conducted well before the phase transition point to avoid any effects of superfluid and Mott insulator states on the atomic lifetime. The experimental data of hold time versus normalized atom numbers at different lattice depths are illustrated in Figure 3a. The experimental data were fitted using Equation (1), and the time at which the atom number decreased to e^{-1} was taken as the effective lifetime in the optical lattice. The dashed line indicates the position where the number of atoms dropped to e^{-1} . As the lattice depth increased from 1.66 Er to 6.34 Er, the effective lifetime of the excited electronic $|F = 2, m_F = 0\rangle$ state gradually decreased. The times at different lattice depths, together with the decay fitting, are shown in Figure 3b. It can be observed that the effective lifetime of atoms decreased with increasing lattice depth, but it was still higher than the effective lifetime in the ODT under the same state.

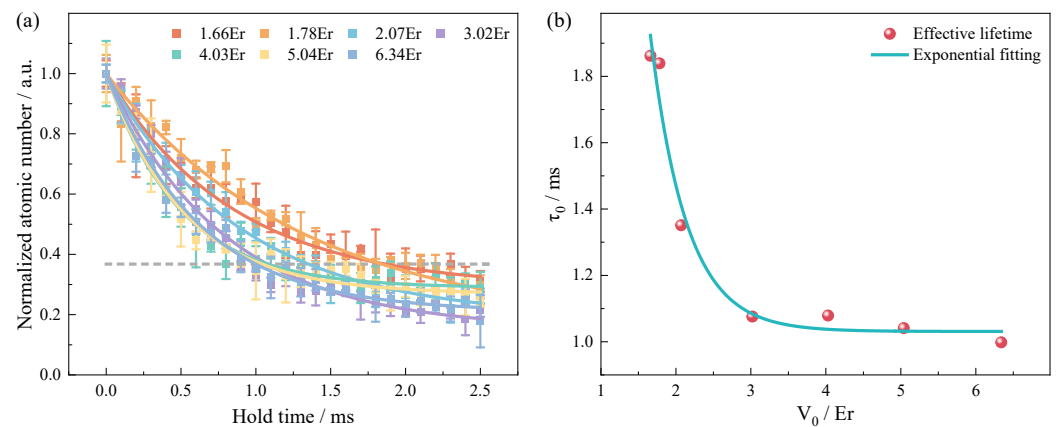


Figure 3. (a) Data points with different colors represent the normalized atomic number at various lattice depths, and the corresponding colored curves represent the exponential fits. (b) The effective lifetime is plotted against different lattice depths, with the solid line indicating an exponential decay fit. For lattice depths of 1.66 Er, 1.78 Er, 2.07 Er, 3.02 Er, 4.03 Er, 5.04 Er, and 6.34 Er, the corresponding effective lifetimes are 1.862 ms, 1.839 ms, 1.351 ms, 1.076 ms, 1.079 ms, 1.041 ms, and 0.998 ms, respectively.

3. Discussion

To evaluate the quality of the fit, we utilized the coefficient of determination, R^2 , which indicates the proportion of variance in the dependent variable that is predictable from the independent variable. The value of R^2 ranges from 0 to 1, with values closer to 1 indicating a better fit of the theoretical model to the data. The formula for calculating R^2 can be described as

$$R^2 = 1 - \frac{SSE}{SST}, \tag{2}$$

where SSE is the sum of the squared residuals of the regression model and SST is the total variance in the dependent variable. The R^2 values for the fitting curves shown in Figures 2 and 3a were both above 0.99, indicating a high degree of fit and reliable experimental results.

Analysis of the lifetimes of the three states in the ODT revealed that the $|F = 2, m_F = -2\rangle$ state had the longest lifetime, followed by the $|F = 2, m_F = 0\rangle$ and $|F = 2, m_F = -1\rangle$. The particularly long lifetime of the $|F = 2, m_F = -2\rangle$ state may be due to the different spontaneous emission rates of the various Zeeman sublevels. According to the selection rules for transitions under the Zeeman effect, $\Delta m_F = 0, \pm 1$, the scattering cross-sections for transitions between different Zeeman sublevels were not the same, leading to different spontaneous emission rates and average lifetimes for the atoms.

By adjusting the loading of the optical lattice, we measured the effective lifetimes of atoms at different lattice depths under a 30 ms ramp, as shown in Figure 3a. The lifetime in the lattice continued to decay exponentially. Notably, the latter half of the fitted curve exhibited intersection points. We attribute these anomalies to the decreased signal-to-noise ratio (SNR) due to the reduced number of atoms, which leads to a decline in data processing accuracy, as well as experimental errors introduced by destructive imaging. Analysis of the experimental data shown in Figure 3b revealed that the effective lifetime of atoms decreased with increasing lattice depth. As the depth of the optical lattice trap increased, the atomic wave functions became more localized, confining the atoms to smaller spatial regions. This localization increased the probability of inter-site atomic collisions, thereby accelerating the decay of atoms within the energy levels and reducing their effective lifetimes. Lattice depth is proportional to volume density and inversely proportional to atomic lifetime [26], further supporting our conclusions. In addition, compared to the lifetime of atoms in the $\text{Na } 3p^2P_{3/2}$ state, the lifetime of atoms in the $3^2S_{1/2}|F = 2\rangle$ state showed a significant enhancement, offering broader advantages for quantum operations involving the $|F = 2\rangle$ state.

4. Conclusions

In this study, we achieved the coherent coupling of the $|F = 1, m_F = -1\rangle$ state to different Zeeman sublevels of the $|F = 2\rangle$ state using microwaves and measured the effective lifetimes of atoms in the $|F = 2, m_F = 0\rangle$, $|F = 2, m_F = -1\rangle$, and $|F = 2, m_F = -2\rangle$ states in the ODT as 0.844 ms, 0.781 ms, and 12.302 ms, respectively. Additionally, we investigated the effective lifetimes of the $|F = 2, m_F = 0\rangle$ state of the Na atoms in the lattice at different trap depths and found that the effective lifetime of atoms decreases with increasing lattice depth. The experimental results obtained in this study provide an important temporal foundation for further quantum simulation operations, demonstrating the superiority of optical lattice loading over ODT loading in terms of atomic lifetimes. Furthermore, this work lays an experimental foundation for further research into the strength and nature of atomic interactions in superfluid and Mott insulator states, as well as non-equilibrium dynamics of atoms after quenching the lattice potential or magnetic field.

Author Contributions: Conceptualization, X.W.; methodology, X.W.; software, X.W.; validation, Y.Q. and J.J.; formal analysis, W.L. and J.W.; investigation, Y.L. and V.S.; data curation, J.M.; writing—original draft preparation, X.W.; writing—review and editing, W.L. and J.W.; visualization, W.L.; supervision, J.W.; project administration, J.W.; funding acquisition, J.W. All authors have read and agreed to the published version of the manuscript.

Funding: This work was supported by the Innovation Program for Quantum Science and Technology (Grant No. 2021ZD0302103), the National Natural Science Foundation of China (Grant Nos. 62325505, 62020106014, 62175140, 62475138, 92165106, and 12104276), the Applied Basic Research Project of

Shanxi Province (Grant No. 202203021224001), and the Graduate Education Innovation Project of Shanxi Province (Grant No. 2024KY019).

Institutional Review Board Statement: Not applicable.

Informed Consent Statement: Not applicable.

Data Availability Statement: Data underlying the results presented in this paper are not publicly available at this time but may be obtained from the authors upon reasonable request.

Conflicts of Interest: The authors declare no conflicts of interest.

References

1. Weber, T.; Herbig, J.; Mark, M.; Nägerl, H.C.; Grimm, R. Bose-Einstein condensation of cesium. *Science* **2003**, *299*, 232–235.
2. Takasu, Y.; Maki, K.; Komori, K.; Takano, T.; Honda, K.; Kumakura, M.; Yabuzaki, T.; Takahashi, Y. Spin-singlet Bose-Einstein condensation of two-electron atoms. *Phys. Rev. Lett.* **2003**, *91*, 040404.
3. Roati, G.; Zaccanti, M.; d’Errico, C.; Catani, J.; Modugno, M.; Simoni, A.; Inguscio, M.; Modugno, G. ^{39}K Bose-Einstein condensate with tunable interactions. *Phys. Rev. Lett.* **2007**, *99*, 010403.
4. Winkler, K.; Thalhammer, G.; Lang, F.; Grimm, R.; Hecker Denschlag, J.; Daley, A.; Kantian, A.; Büchler, H.; Zoller, P. Repulsively bound atom pairs in an optical lattice. *Nature* **2006**, *441*, 853–856.
5. Hempel, C.; Maier, C.; Romero, J.; McClean, J.; Monz, T.; Shen, H.; Jurcevic, P.; Lanyon, B.P.; Love, P.; Babbush, R.; et al. Quantum chemistry calculations on a trapped-ion quantum simulator. *Phys. Rev. X* **2018**, *8*, 031022.
6. Bluvstein, D.; Levine, H.; Semeghini, G.; Wang, T.T.; Ebadi, S.; Kalinowski, M.; Keesling, A.; Maskara, N.; Pichler, H.; Greiner, M.; et al. A quantum processor based on coherent transport of entangled atom arrays. *Nature* **2022**, *604*, 451–456.
7. Daley, A.J.; Bloch, I.; Kokail, C.; Flannigan, S.; Pearson, N.; Troyer, M.; Zoller, P. Practical quantum advantage in quantum simulation. *Nature* **2022**, *607*, 667–676.
8. Flannigan, S.; Pearson, N.; Low, G.H.; Buyskikh, A.; Bloch, I.; Zoller, P.; Troyer, M.; Daley, A.J. Propagation of errors and quantitative quantum simulation with quantum advantage. *Quantum Sci. Technol.* **2022**, *7*, 045025.
9. Liu, J.; Wang, Y.; Tu, B.; Huang, L.; Si, R.; Li, J.; Zhang, M.; Fu, Y.; Zou, Y.; Yao, K. Lifetime measurement of the $3d^{92}\text{D}_{3/2}$ metastable level in Mo^{15+} at an electron beam ion trap. *Chin. Phys. B* **2023**, *32*, 103201.
10. Oates, C.W.; Vogel, K.; Hall, J.L. High precision linewidth measurement of laser-cooled atoms: Resolution of the $\text{Na } 3p^2P_{3/2}$ lifetime discrepancy. *Phys. Rev. Lett.* **1996**, *76*, 2866.
11. Simsarian, J.; Orozco, L.A.; Sprouse, G.; Zhao, W. Lifetime measurements of the 7 p levels of atomic francium. *Phys. Rev. A* **1998**, *57*, 2448.
12. Gibbons, M.J.; Kim, S.Y.; Fortier, K.M.; Ahmadi, P.; Chapman, M.S. Achieving very long lifetimes in optical lattices with pulsed cooling. *Phys. Rev. A-At. Mol. Opt. Phys.* **2008**, *78*, 043418.
13. Pelisson, S.; Messina, R.; Angonin, M.C.; Wolf, P. Lifetimes of atoms trapped in an optical lattice in proximity of a surface. *Phys. Rev. A-At. Mol. Opt. Phys.* **2013**, *88*, 013411.
14. Saglamyurek, E.; Lutz, T.; Veissier, L.; Hedges, M.P.; Thiel, C.W.; Cone, R.L.; Tittel, W. Efficient and long-lived Zeeman-sublevel atomic population storage in an erbium-doped glass fiber. *Phys. Rev. B* **2015**, *92*, 241111.
15. Magalhães, K.M.F.; De Oliveira, A.; Zanon, R.; Bagnato, V.S.; Marcassa, L.G. Lifetime determination of high excited states of ^{85}Rb using a sample of cold atoms. *Opt. Commun.* **2000**, *184*, 385–389.
16. Mack, M.; Grimm, J.; Karlewski, F.; Sárkány, L.; Hattermann, H.; Fortágh, J. All-optical measurement of Rydberg-state lifetimes. *Phys. Rev. A* **2015**, *92*, 012517.
17. de Oliveira, A.L.; Mancini, M.W.; Bagnato, V.S.; Marcassa, L.G. Measurement of Rydberg-state lifetimes using cold trapped atoms. *Phys. Rev. A* **2002**, *65*, 031401.
18. Nascimento, V.; Caliri, L.; De Oliveira, A.; Bagnato, V.S.; Marcassa, L.G. Measurement of the lifetimes of S and D states below $n = 31$ using cold Rydberg gas. *Phys. Rev. A—At. Mol. Opt. Phys.* **2006**, *74*, 054501.
19. Caliri, L.L.; Marcassa, L.G. Reply to “Comment on ‘Measurement of the lifetimes of S and D states below $n = 31$ using cold Rydberg gas’”. *Phys. Rev. A—At. Mol. Opt. Phys.* **2007**, *75*, 066503.
20. Beterov, I.; Ryabtsev, I.; Tretyakov, D.; Entin, V. Quasiclassical calculations of blackbody-radiation-induced depopulation rates and effective lifetimes of Rydberg nS , nP , and nD alkali-metal atoms with $n \leq 80$. *Phys. Rev. A—At. Mol. Opt. Phys.* **2009**, *79*, 052504.
21. Jing, H.; Ye, S.W.; Dai, C.J. Lifetimes of Rydberg states of Eu atoms. *Chin. Phys. B* **2015**, *24*, 013203.
22. Heo, M.S.; Wang, T.T.; Christensen, C.A.; Rvachov, T.M.; Cotta, D.A.; Choi, J.H.; Lee, Y.R.; Ketterle, W. Formation of ultracold fermionic NaLi Feshbach molecules. *Phys. Rev. A—At. Mol. Opt. Phys.* **2012**, *86*, 021602.
23. Jachymski, K.; Gronowski, M.; Tomza, M. Collisional losses of ultracold molecules due to intermediate complex formation. *Phys. Rev. A* **2022**, *106*, L041301.

24. Schymik, K.N.; Pancaldi, S.; Nogrette, F.; Barredo, D.; Paris, J.; Browaeys, A.; Lahaye, T. Single atoms with 6000-second trapping lifetimes in optical-tweezer arrays at cryogenic temperatures. *Phys. Rev. Appl.* **2021**, *16*, 034013.
25. Hölzl, C.; Götzelmann, A.; Pultinevicius, E.; Wirth, M.; Meinert, F. Long-lived circular Rydberg qubits of alkaline-earth atoms in optical tweezers. *Phys. Rev. X* **2024**, *14*, 021024.
26. Zhai, Y.; Yue, X.; Wu, Y.; Chen, X.; Zhang, P.; Zhou, X. Effective preparation and collisional decay of atomic condensates in excited bands of an optical lattice. *Phys. Rev. A—At. Mol. Opt. Phys.* **2013**, *87*, 063638.
27. Shui, H.; Lai, C.K.; Yu, Z.; Tian, J.; Wu, C.; Chen, X.; Zhou, X. Optimal lattice depth on lifetime of D-band ultracold atoms in a triangular optical lattice. *Opt. Express* **2023**, *31*, 26599–26609.
28. Chen, Z.; Tang, T.; Austin, J.; Shaw, Z.; Zhao, L.; Liu, Y. Quantum quench and nonequilibrium dynamics in lattice-confined spinor condensates. *Phys. Rev. Lett.* **2019**, *123*, 113002.
29. Qiu, L.Y.; Liang, H.Y.; Yang, Y.B.; Yang, H.X.; Tian, T.; Xu, Y.; Duan, L.M. Observation of generalized Kibble-Zurek mechanism across a first-order quantum phase transition in a spinor condensate. *Sci. Adv.* **2020**, *6*, eaba7292.
30. Guo, S.A.; Wu, Y.K.; Ye, J.; Zhang, L.; Lian, W.Q.; Yao, R.; Wang, Y.; Yan, R.Y.; Yi, Y.J.; Xu, Y.L.; et al. A site-resolved two-dimensional quantum simulator with hundreds of trapped ions. *Nature* **2024**, *630*, 613–618.
31. Feng, L.; Huang, Y.Y.; Wu, Y.K.; Guo, W.X.; Ma, J.Y.; Yang, H.X.; Zhang, L.; Wang, Y.; Huang, C.X.; Zhang, C.; et al. Realization of a crosstalk-avoided quantum network node using dual-type qubits of the same ion species. *Nat. Commun.* **2024**, *15*, 204.
32. Peng, P.; Zhang, Z.; Fan, Y.; Yin, G.; Mao, D.; Chen, X.; Xiong, W.; Zhou, X. Atomic transport dynamics in crossed optical dipole trap. *Chin. Phys. B* **2024**, *33*, 073701.
33. Lewenstein, M.; Sanpera, A.; Ahufinger, V.; Damski, B.; Sen, A.; Sen, U. Ultracold atomic gases in optical lattices: Mimicking condensed matter physics and beyond. *Adv. Phys.* **2007**, *56*, 243–379.
34. Bloch, I.; Dalibard, J.; Zwerger, W. Many-body physics with ultracold gases. *Rev. Mod. Phys.* **2008**, *80*, 885–964.
35. Liu, W.; Zheng, N.; Wang, X.; Xu, J.; Li, Y.; Sovkov, V.B.; Li, P.; Fu, Y.; Wu, J.; Ma, J.; et al. Fast, simple, all-optical production of sodium spinor condensates. *J. Phys. B At. Mol. Opt. Phys.* **2021**, *54*, 155501.
36. Black, A.T.; Gomez, E.; Turner, L.D.; Jung, S.; Lett, P.D. Spinor dynamics in an antiferromagnetic spin-1 condensate. *Phys. Rev. Lett.* **2007**, *99*, 070403.
37. Tsui, T.; Wang, Y.; Subhankar, S.; Porto, J.V.; Rolston, S. Realization of a stroboscopic optical lattice for cold atoms with subwavelength spacing. *Phys. Rev. A* **2020**, *101*, 041603.
38. Liu, W.; Zheng, N.; Jian, J.; Tian, L.; Wu, J.; Li, Y.; Fu, Y.; Li, P.; Sovkov, V.; Ma, J.; et al. Superfluid to Mott-insulator transition in a one-dimensional optical lattice. *Chin. Phys. B* **2022**, *31*, 073702.

Disclaimer/Publisher’s Note: The statements, opinions and data contained in all publications are solely those of the individual author(s) and contributor(s) and not of MDPI and/or the editor(s). MDPI and/or the editor(s) disclaim responsibility for any injury to people or property resulting from any ideas, methods, instructions or products referred to in the content.